Bollettino di Geofisica Teorica ed Applicata Vol. 62, n. 1, pp. 101-118; March 2021
DOI 10.4430/bgta0335

Contribution of aeromagnetic cartography and lithostratigraphic studies to the identification of blind faults and the Cambrian deposits geometry in Jbel Saghro (eastern Anti-Atlas, Morocco)

A. Idrissi[1], M. Saadi[1], A. Manar[2], Y. Astati[3], L. Harrouchi[4] and J.E. Nacer[5]

[1] *Department of Earth Sciences, Faculty of Sciences, Mohamed V University, Rabat, Morocco*
[2] *Ministry of Energy, Mines and Environment, Rabat, Morocco*
[3] *National Office of Hydrocarbons and Mines, Rabat, Morocco*
[4] *Sahara Geology Laboratory, Kasdi Merbah University, Ouargla, Algeria*
[5] *Nuclear Research Center of Draria, Algiers, Algeria*

(Received: 12 March 2020; accepted: 9 June 2020)

ABSTRACT The study area corresponds to the Jbel Saghro mountain range located in the Moroccan eastern Anti-Atlas. The area landscape shows a Palaeozoic cover, overlying a Neoproterozoic basement. The Cambrian series present lateral thinning from east to west; this thinning is related to the rifting events occurring during the late Neoproterozoic-Cambrian period. The rifting transformed the Anti-Atlas into horsts and grabens. The grabens recorded important sedimentation through the Lower and Middle Cambrian, while at the horsts, it remained reduced. Four lithological sections were examined: Boumalne, Imiter, Taghazout West, and Taghazout, distributed respectively from west to east. The Lower Cambrian is absent in the Boumalne and Imiter, while the Middle Cambrian series show a thickening from west to east. The rifting was generalised in the Anti-Atlas domain, and produced by NE-SW trending faults. The aim of this work is to identify the deepening of these faults, relying on field and geomagnetic examinations. Several treatments were applied to the Jbel-Saghro residual magnetic field map: reduction-to-pole, horizontal gradient, and Euler's deconvolution. Numerous faults were revealed, including a NE-SW trending system interpreted as Cambrian rifting faults, and a NW-SE trending system described as late Neoproterozoic extension faults. These fault systems are considered responsible for the thickness variations of the Cambrian series along the northern flank of Jbel Saghro.

Key words: Cambrian, aeromagnetic data, rifting, graben, horst, Jbel Saghro, eastern Anti-Atlas.

1. Introduction

The Jbel Saghro has been the subject of many researches investigating its complicated geodynamic evolution. After the Pan-African orogeny, a post-orogenic distension was triggered (Leblanc and Lancelot, 1980), and continued until the Lower Cambrian period. A NW - SE trending extension took place, leading to an architecture of horsts and grabens throughout the entire Anti-Atlas (Soulaimani *et al*., 2003; Burkhard *et al*., 2006; Gouiza *et al*., 2017). This architecture

influenced the behaviour and the establishment of Cambrian sedimentation: the absence of the Lower Cambrian series along the northern flank of the Jbel Saghro, and the decrease of the thickness of Middle Cambrian deposits in its north-western part.

Previous works in the Saghro area focused on field observations to describe the Late Neoproterozoic-Cambrian rifting (Raddi *et al*., 2007; Pouclet *et al*., 2018; Hejja *et al*., 2020). Baidder (2007) described the influence of the rifting on the Cambrian sedimentation, assuming the existence of a ditch at the eastern region of the Jbel Saghro. For a better understanding of the structural parameters of the rifting event, this study presents the contribution of field investigations and aeromagnetic cartography. The depths of all faults deduced by geophysical methods indicate that they are all blind faults, which proves the efficacy of the aeromagnetic examination in this study.

The aim of this paper is to explain the hiatus of the Lower Cambrian in the western part of the Jbel Saghro, and to identify the reasons for the sediment thickness variations along the Jbel Saghro northern flank. The results of the field investigation are represented in the cross-sections, illustrating the sedimentological properties of the Lower and Middle Cambrian. The aeromagnetic data treatment results are described by the maps of magnetic faults. The integration of the results led to identifying the supposed responsible faults, and described the connection between the rifting and the sedimentation behaviour in the northern flank of Jbel Saghro.

2. Geographical and geological setting

The Jbel Saghro is located in the north-eastern part of the Moroccan Anti-Atlas Belt (Fig. 1); considering its position on the northern boundary of the West African Craton (Destombes *et al*., 1985), its tectonic history ranges from Pan-African to Alpine event (Gouiza *et al*., 2017).

2.1. Structural setting

The geodynamic history of the Moroccan Anti-Atlas domain during the Late Neoproterozoic - Lower Cambrian period, evidences an extensive system. This system resulted from the sinistral rotation of the West African Craton (Burkhard *et al*., 2006; Baidder, 2007), through the Major Accident of the Anti-Atlas and the South Atlasic Accident (Baidder, 2007). An intra-continental rifting environment was created that structured the Anti-Atlas in high and low zones (Soulaimani *et al*., 2003; Burkhard *et al*., 2006). The rifting event is also testified by the peralkaline felsic magmatism generated at that time (Bea *et al*., 2016).

In the western Anti-Atlas, the extension is oriented NW-SE (Benssaou and Hamoumi, 2003) and the directions of the resulting faults vary between N-S to NNE-SSW (N20°) dipping essentially toward the west, and NE-SW (N40° - N50°) dipping to the NNW (Algouti *et al*., 2001).

In the central Anti-Atlas, the extension is oriented NW-SE, controlled by various normal faults: E-W faults, N70° normal faults, and N110° sinistral transtensive faults (Soulaimani *et al*., 2003). In the eastern Anti-Atlas, the faults are normal with a N70° trending and others are NW-SE with sinistral components (Baidder, 2007). The extension had a NW-SE orientation as in the central Anti-Atlas.

The structuration of the Anti-Atlas in horsts and grabens (Soulaimani *et al*., 2003) led to lateral variations of the Cambrian series in term of facies and thickness.

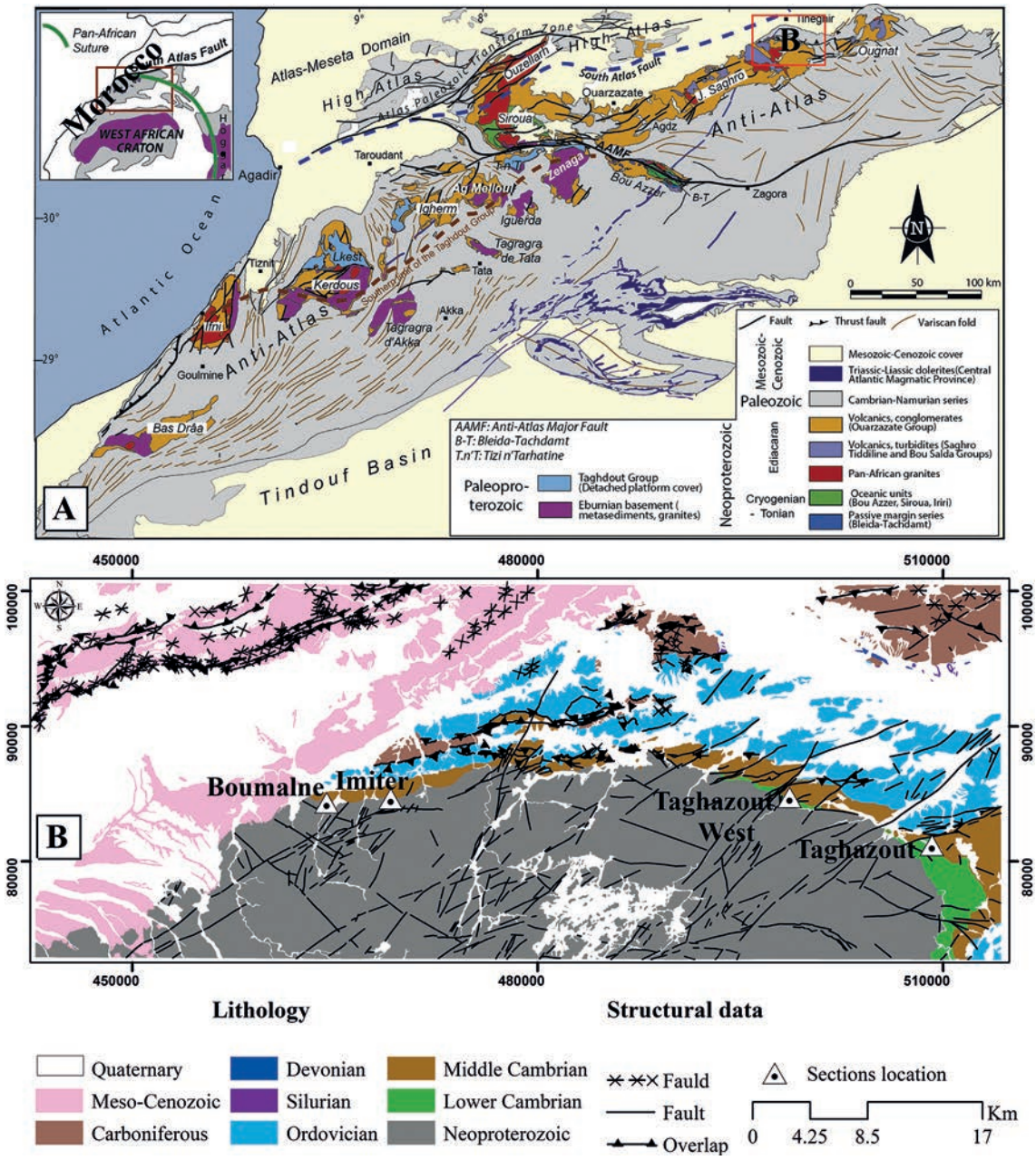

Fig. 1 - Geographical and geological position of the study area: A) map of the Anti-Atlas Belt of Morocco showing generalised geological features. Inset: location of the Jbel Saghro in relation to the Anti-Atlas Belt (Gasquet *et al*., 2008, modified by Soulaimani *et al*., 2018); B) digitised geological map derived from geological maps of Boumalne, Imiter, and Taghazout (scale 1:50,000), showing the geological features of the study area (lithology and structural elements) and the location of the lithostratigraphic sections at the north-eastern flank of the Jbel Saghro.

The low areas recorded significant sedimentation during the Lower Cambrian transgression, while the high areas remained emerged. As the Middle Cambrian transgression took place (Choubert, 1946), the sea more or less invaded the entire Moroccan relief, triggering the deposition of paradoxides schists and the Tabanite sandstones.

2.2. Lithostratigraphic setting

The stratigraphy of the Anti-Atlas Cambrian sedimentation is dated by the trilobite fauna, and distributed on various lithostratigraphic groups (Piqué *et al*., 2007). The Lower Cambrian is composed of transgressive limestones and clays, followed by regressive sandstones. The thickness of this formation decreases from the Anti-Atlas western regions to the eastern ones. The Middle Cambrian comprises the paradoxides schists group made up of pelitic facies, and followed by the regressive Tabanite sandstones (Choubert, 1946).

During the Late Cambrian, the Anti-Atlas domain was emerged (Destombes and Feist, 1987; Ennih and Liégeois, 2001). However, the Late Cambrian was identified locally at the top of the Tabanite sandstones in the Foum Zguid region (central Anti-Atlas), by Périgondowanien Ollentela Africana trilobites, revealing then, for the first time in Africa, the existence of the Late Cambrian (Destombes and Feist, 1987).

The Cambrian sediments are followed by the Ordovician formations, that lie above the Tabanite group; this formation contains several sequences of argillites alternating with sandstones (Choubert, 1946; Marante, 2008).

Unlike the rest of the Anti-Atlasic Belt, the eastern Anti-Atlas generally registers a hiatus of Lower Cambrian (Fig. 2) (Gasquet *et al*., 2005), except for some eastern and southern areas of the Jbel Saghro, where the Lower Cambrian deposits are poorly recorded.

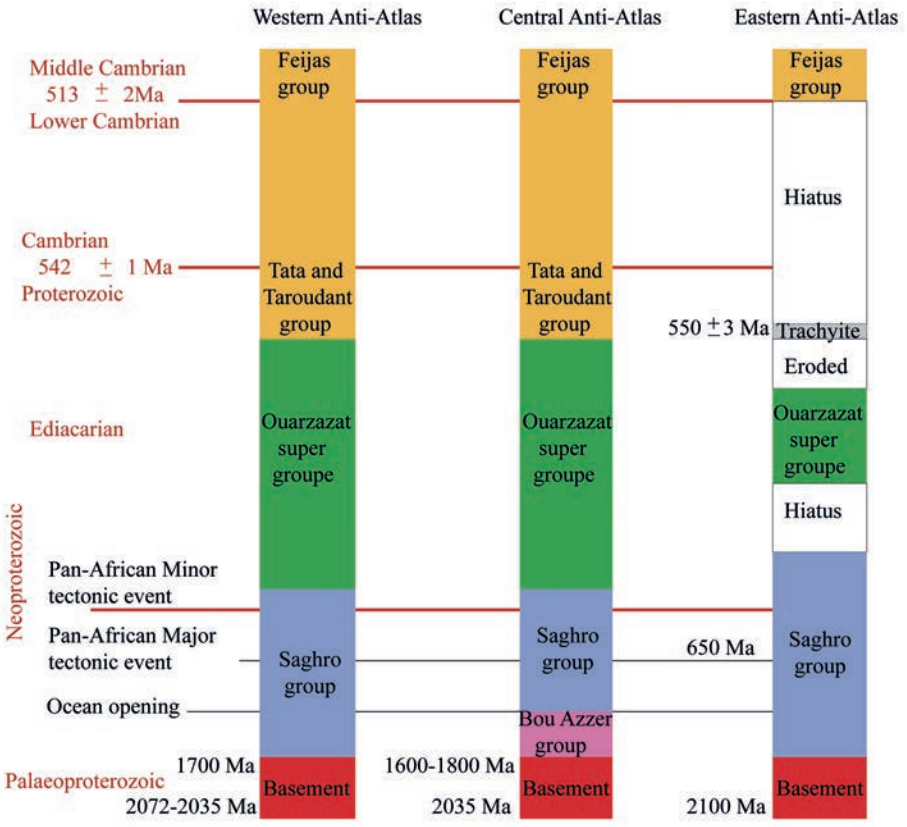

Fig. 2 - Anti-Atlas lithostratigraphy (Gasquet *et al*., 2005).

3. Data sets and methodology

3.1. Field data

The study area displays an interesting dissimilarity of Cambrian deposits and a variation of their thickness. One possible reason behind this disparity is the geodynamic history of the Anti-Atlas domain throughout the Late Neoproterozoic - Cambrian period. Therefore, we carried out several field missions to establish lithostratigraphic sections, and to analyse the different faulting systems in the region. The anterior sedimentation limited our investigation, hence, we led the study using the aeromagnetic mapping, to expose any buried geological structures and especially faults.

3.2. Aeromagnetic data

The aeromagnetic maps used in this work were obtained from the Moroccan Ministry of Energy, Mines and Environment (scale: 1:100,000). The aeromagnetic maps were acquired in 1977, from two magnetic surveys flown at different elevations. The north-western part of the study area is covered by the first survey at 4300 m height above mean sea level. The flight lines and the tie lines were respectively oriented N135° and N45°. The lines spacing was between 3000 and 3500 m for flight lines and between 10,000 to 15,000 m for tie lines. The second survey covers the rest of the northern flank of Jbel Saghro. The plane flew along N135° oriented lines and N45° directed tie lines at an elevation of 2600 m above mean sea level. The spacing was 3000 m for the flight lines and ranging from 10000 to 15000 m for the tie lines (Fig. 3). The International Geomagnetic Reference Field (IGRF) for the time of acquisition was removed from the data. The residual magnetic field maps filtered in this study, were previously adjusted and provided in a paper format (parameters: unit = gamma (γ) ($1\gamma = 1$ nT); tilt = 43.49°; declination = - 6.44°).

In order to standardise, both aeromagnetic surveys are combined to 2600 m above mean sea level using the continuation filter, then interpolated using the minimum curvature method within a grid of 750×750 m^2.

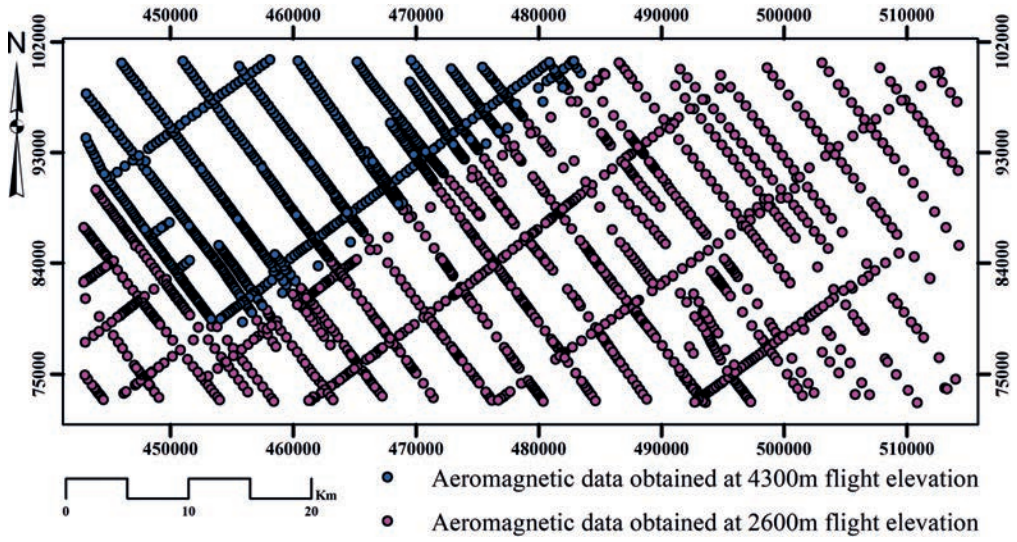

Fig. 3 - Representation of the flight lines and tie lines of the aeromagnetic surveys.

3.3. Methodology

The data was extracted from the maps, following the workflow described in the Fig. 4. The values of the residual magnetic field contours were digitised at the intersection point with the flight lines and tie lines by Arcgis software and transferred onto a regular mesh grid of the Oasis montaj software (Geosoft Inc., 2007).

The database obtained from these procedures, allowed us to produce the residual magnetic field map, using the mapping tools of Oasis montaj software (Geosoft Inc., 2007). The residual map was, then, treated by several mathematical techniques by the same software (Fig. 4).

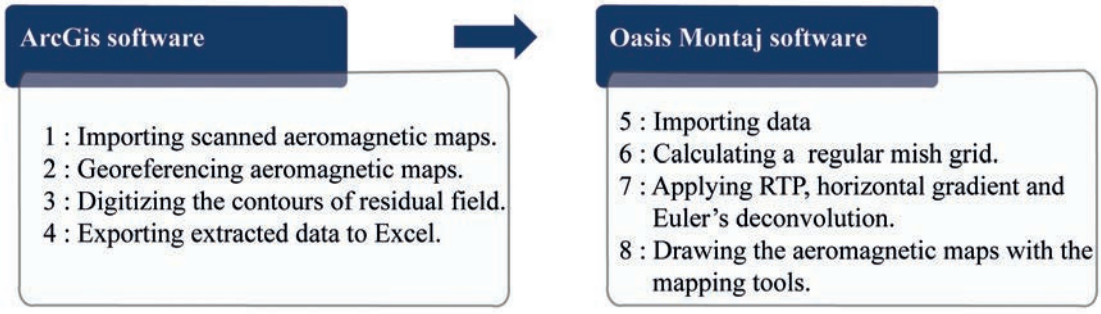

Fig. 4 - Workflow of extraction and treatment of aeromagnetic data.

The first step in the filtering process is to reduce the residual magnetic field map to the pole, in order to locate and delineate the sources of magnetic anomalies (tilt = 43.49°; declination = -6.44°), this operation enables producing the reduced to a pole (RTP) map. The RTP map will be used as the base map for applying conventional mathematical techniques of source edge detection used in aeromagnetism. These techniques are the horizontal gradient and the Euler deconvolution, as described below.

The horizontal gradient is used in structural mapping, it is a strong method in source edge detection (Cordell, 1979; Amiri *et al*., 2011; Azaiez *et al*., 2011; Dufréchou *et al*., 2013; Gabtni *et al*., 2013; Nait Bba *et al*., 2019). In this work, the horizontal gradient has been applied to the RTP grid of the study area, to detect and locate linear structures, identified by sudden variations of the magnetic field (Blakely and Simpson, 1986). The revealed structures can be interpreted as geological contacts or subsurface faults.

The horizontal gradient equation (Cordell and Grauch, 1985) is written as:

$$GH(x,y) = \sqrt{\left(\frac{dT}{dx}\right)^2 + \left(\frac{dT}{dy}\right)^2} \qquad (1)$$

where T is the total field reduced to the pole, dx and dy are the first horizontal derivatives following respectively x and y.

Moreover, the Euler's deconvolution allows locating and delineating the causative magnetic bodies, dykes, geological contacts, cylinders, and spheres according to the involved structural index [*SI*: Reid *et al*. (1990), see Table 1]. With a *SI* equal to zero, we were able to highlight the depth of magnetic faults, and, thus, to compile the magnetic lineaments map of the study

area. Thompson (1982) demonstrated that Euler's homogeneity equation can be written (Table 2) as:

$$N\,(B - T) = \frac{(x - x0)\partial T}{\partial x} + \frac{(y - y0)\partial T}{\partial y} + \frac{(z - z0)\partial T}{\partial z} \quad . \qquad (2)$$

Table 1 - *N* values by source geometry (Reid *et al*., 1990).

Geometric source	*N* (magnetism)
Sphere	3
Vertical cylinder	2
Cylindre horizontal Horizontal cylinder	2
Dyke / Sill	1
Contact	0

Table 2 - Terms of the Euler deconvolution equation.

Equation terms	Significance
x_0, y_0, z_0	Position of the magnetic sources
x, *y*, *z*	Observation point position
T	Total field detected at (*x*, *y*, *z*)
B	Regional value of the total field
N	Degree of homogeneity often referred to as the structural index (SI) which characterizes the type of source

4. Results and interpretation

4.1. Lithostratigraphic study

The lithostratigraphic sections in this study were acquired during the sedimentary survey in the regions of Boumalne, Imiter, and Taghazout, located on the north-eastern flank of Jbel Saghro (Fig. 1B).

The thickness of the Lower Cambrian deposits decreases in the Taghazout area from the east to the west with a total disappearance in the Boumalne and Imiter areas. Instead, the deposits of the Middle Cambrian show similarity in terms of facies and a difference of thickness.

4.1.1. Lower Cambrian

At the eastern region of the Jbel Saghro, the Lower Cambrian is subdivided into three units.

In the Taghazout section (Fig. 5d), the basal unit corresponds to a 120 m alternating polygenic and polymetric conglomeratic sediment. The conglomerates have a Gully base and are constituted of andesitic fragments, cemented together by a carbonaceous matrix. This set is overlaid by an association of calcarenite and centimetric purplish clay levels. The basal unit presents graded sediment, the grain size decreased from coarse to fine toward the top. The unit is topped by a centimetric purplish clay levels.

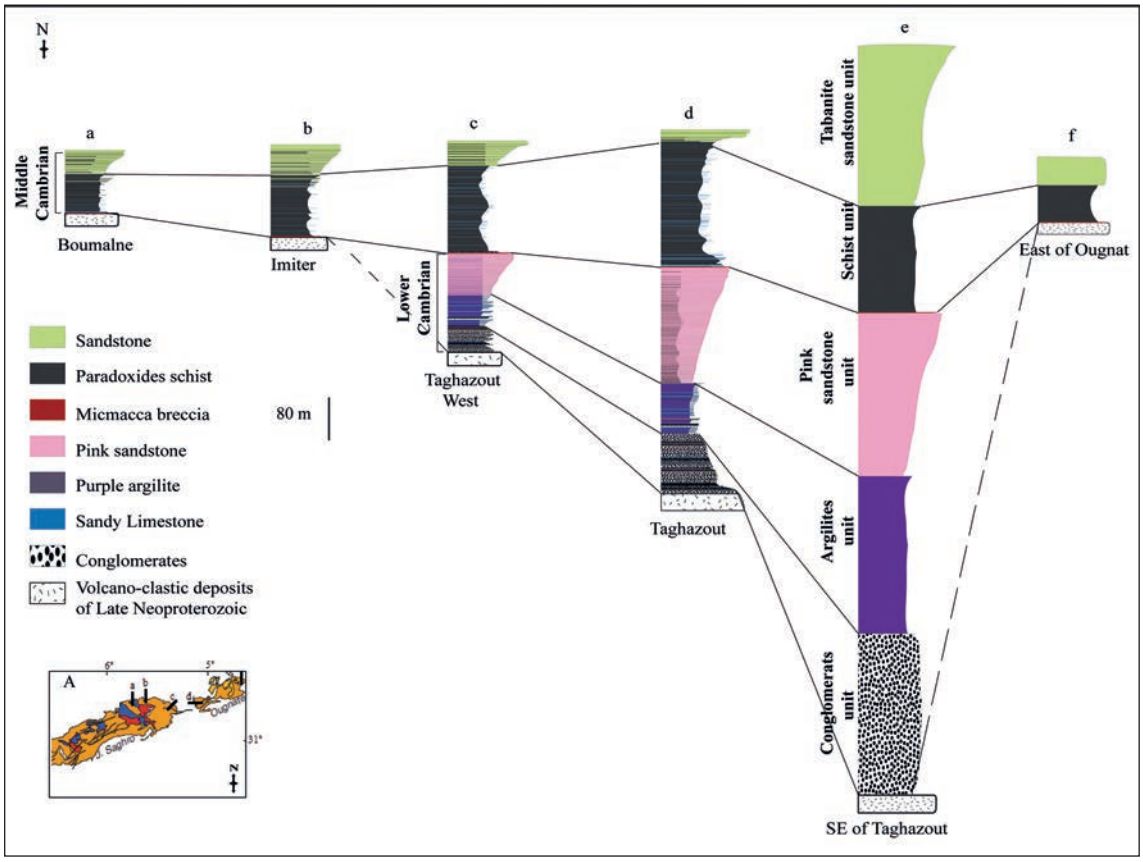

Fig. 5 - Lateral correlation between lithostratigraphic sections of the Lower and Middle Cambrian series, showing the variation of thickness and facies between the Boumalne, Imiter, Taghazout West, and Taghazout sections, in addition to the two sections made respectively east of Taghazout and east of Ougnat by Baidder (2007). In the inset, the position of the lithostratigraphic sections in relation to Jbel Saghro and Ougnat Massif.

The middle unit comprises 100-m-thick, red to purplish clay deposits, with alternating centimetric levels of sand and sandstone. The upper unit is 200 m thick and corresponds to decimetric pink sandstone bars that pass to metric benches towards the top. These benches show centimetric conglomeratic levels, clay lenses, oblique stratification, and current ripples.

The Taghazout West section (Fig. 5c) is similar to the previous section in terms of the identified facies. The section illustrates the basal unit by a 50-m alternating polygenic and polymetric conglomeratic deposit (centimetric to decametric), also constituted of andesitic fragments. This set is normal graded, and overlaid by an alternation of thin calcarenite and purplish clay levels. The middle unit comprises 14-m-thick purplish clay deposits, alternating with centimetric levels of sand and sandstone.

The upper unit is 70 m thick and constituted of decametric to metric pink sandstone benches. The former show thin conglomeratic levels, widespread clay lenses, oblique stratification and current ripples at the top.

At the base of the Imiter and Boumalne sections (Figs. 5a and 5b), the Lower Cambrian deposits are absent; the Middle Cambrian deposits lie directly on the upper Neoproterozoic volcano-clastic series.

4.1.1. Middle Cambrian

The Taghazout lithostratigraphic log (Fig. 5d) illustrates the Middle Cambrian with two sedimentary units. The basal unit comprises green-schist known as "schistes à paradoxides", transgressing on the Lower Cambrian pink sandstones, following a reference level of Micmacca Breccia. This latter is cemented by a sandy-calcareous matrix, topped by a 20-cm conglomerate with fragments of sandstone and limestone. The schist formation is trilobites-rich, with 190 m of thickness, and along which centimetric limestones lenses alternate, and become more frequent towards the top.

The second unit is 20-m-thick yellowish fine sandstone bars, with oblique stratification, alternating with centimetric to decimetric clay levels. The sandstone bars thickness increases from the base to the top.

The Taghazout West log (Fig. 5c) comprises at the base a 140 m of green-schist intercalating with fine limestone beds towards the top of the unit. This set is followed by the Tabanite formation, represented by a 30-m-thick bar of sandstones bars.

Further to the west, the Palaeozoic cover deposits in the Imiter section (Fig. 5b) begins with the Middle Cambrian formations, which unconformably overlie the Neoproterozoic basement, following a transgressive unconformity, consisting of conglomeratic deposits, Micmacca Breccia, and stromatolitic limestone. The thickness of the green-schist series in this region is 90 m, topped by a 25 m of alternating sandy-limestones levels. As in the Taghazout region, the second unit of Middle Cambrian deposits is represented by 50 m of sandstone. The sandstone bars are thicker from the base to the top of the unit, and they can reach a thickness of 20 m.

The Boumalne zone shows a significant reduction in thickness, compared to the Imiter region (Fig. 6). The deposits of the Middle Cambrian lie on the Neoproterozoic basement through the level of Micmacca Breccia. Similar to the two previous sections, the Boumalne section presents two sedimentary units of Middle Cambrian, the unit of the schists, and the unit of the Tabanite sandstones. The schists are 70 m thick, with centimetric sandy levels along the section, while Tabanite sandstones are present in massive bars of 40 m with local clay lenses along the unit.

4.2. Aeromagnetic data analysis

4.2.1. Residual magnetic field map

Based on airborne data, the residual magnetic field map of the Jbel Saghro, Moroccan Anti-Atlas, has been sketched (Fig. 6).

The residual magnetic field map is plotted using the Minimum Curvature interpolation method; the Oasis montaj software (Geosoft Inc., 2007) was programmed to highlight the low-intensities in blue and the high-intensities in red. The anomalies were detected in different types of form, organization, orientation, and intensities. In fact, this map shows anomalies with variable dimensions and amplitudes, the northern and middle part of the study area are dominated by high anomalous magnetic intensity values, respectively elongated E-W and WNW-ESE. The magnetic gradient decreases from the north to the south, whereas the southern part is characterised by low magnetic intensity values, showing low anomalies oriented E-W, NW-SE and NNE-SSW.

4.2.2. Reduced to pole map

The geometric configuration of magnetic anomalies in two lobes, makes it difficult to analyse and interpret magnetic maps. In order to minimise polarity effects and find the corresponding

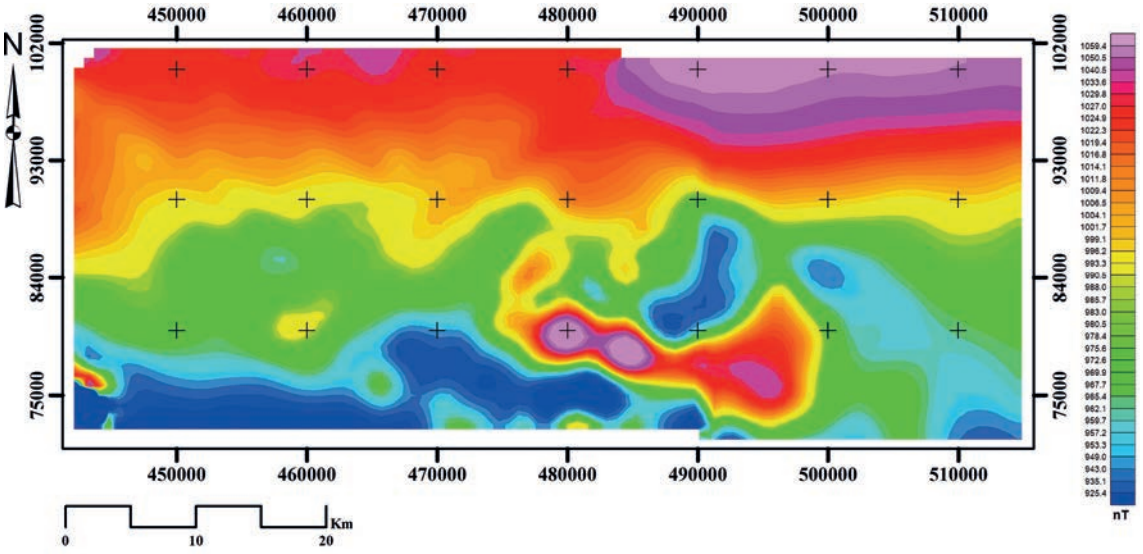

Fig. 6 - Residual magnetic field map of the Jbel Saghro northern flank.

causative sources of magnetic anomalies, Baranov (1957) and Baranov and Naudy (1964) introduced the transformation of reduction to the pole.

The analysis of the magnetic field map reduced to the pole (Fig. 7) reveals a better definition of the magnetic anomalies. The high-intensity anomalies range between 1043 and 1080 nT and are oriented N-S (A1, A2, and A3). Low-intensity anomalies, which are concentrated in the southern part of the map (A4, A5, and A6), trend E-W and N-S.

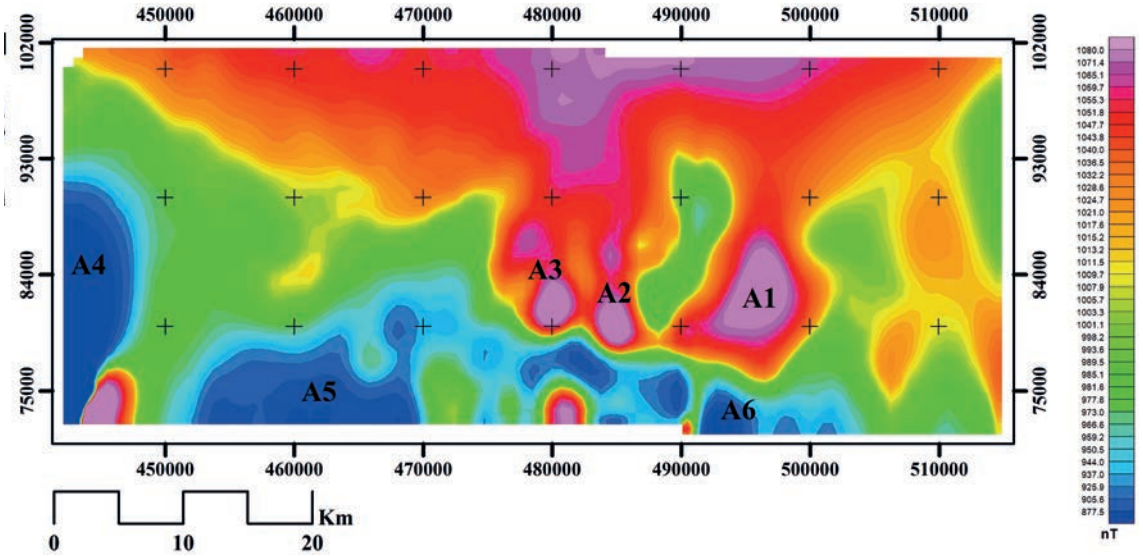

Fig. 7 - Residual magnetic field map reduced to pole of the Jbel Saghro northern flank.

The analysis of the geological Boumalne, Imiter, and Taghazout maps at the scale 1:50,000 shows that the anomalies are located in the highly magnetic basement (Fig. 8), constituted of rhyolites and ignimbrites, tuffs, obsidian and andesitic veins (Buggisch and Flügel, 1988), metamorphic and sedimentary rocks (Burkhard *et al*., 2006).

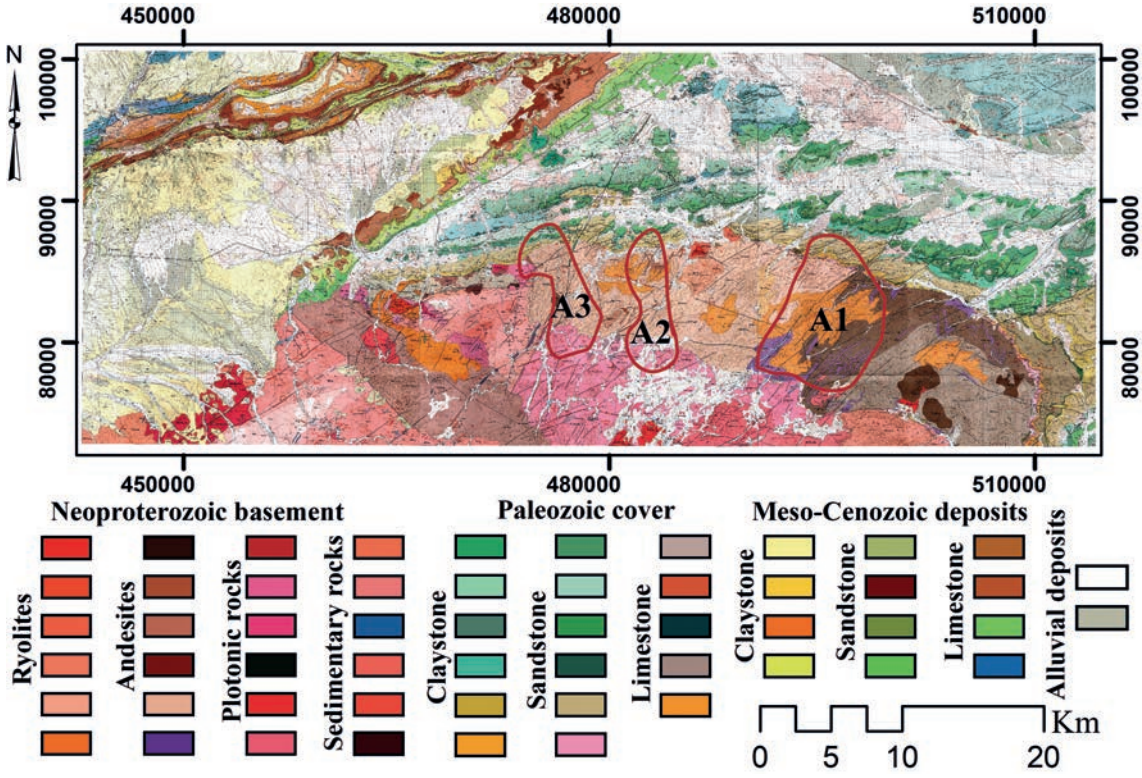

Fig. 8 - Geological map of the northern flank of Jbel Saghro (scale 1:50,000), showing the distribution of the volcano-clastic Neoproterozoic basement, the Palaeozoic cover and the Meso-Cenozoic deposits, and the location of the anomalies A1, A2, and A3 in the Neoproterozoic basement.

4.2.3. Horizontal gradient map

The horizontal gradient is a useful parameter for the localisation of contacts and the magnetic sources limits on the horizontal plane (Bournas, 2001; Harrouchi, 2017). It is also useful in major subsurface discontinuities detection. The horizontal gradient map is produced via the Source Edge Detection (SED) filter, the SED filter is also used to determine the magnetic faults directions (Fig. 10).

On the map of the horizontal gradient (Fig. 9), the anomalies are presented in quasi-linear forms; the intense anomalies are concentrated in a highly magnetic Neoproterozoic basement, while the low anomalies are located on a moderate to low magnetisation Palaeozoic to Meso-Cenozoic cover. The horizontal gradient map of the study area reveals a set of lineaments of different directions; the directions are given below in order of dominance:

- the NW-SE are located in the north-western and the eastern part of the map. The previous works linked these directions with the corresponding tectonic events in the eastern Anti-Atlas. Mokhtari (1993) matched the NW-SE family to the extension of the Upper

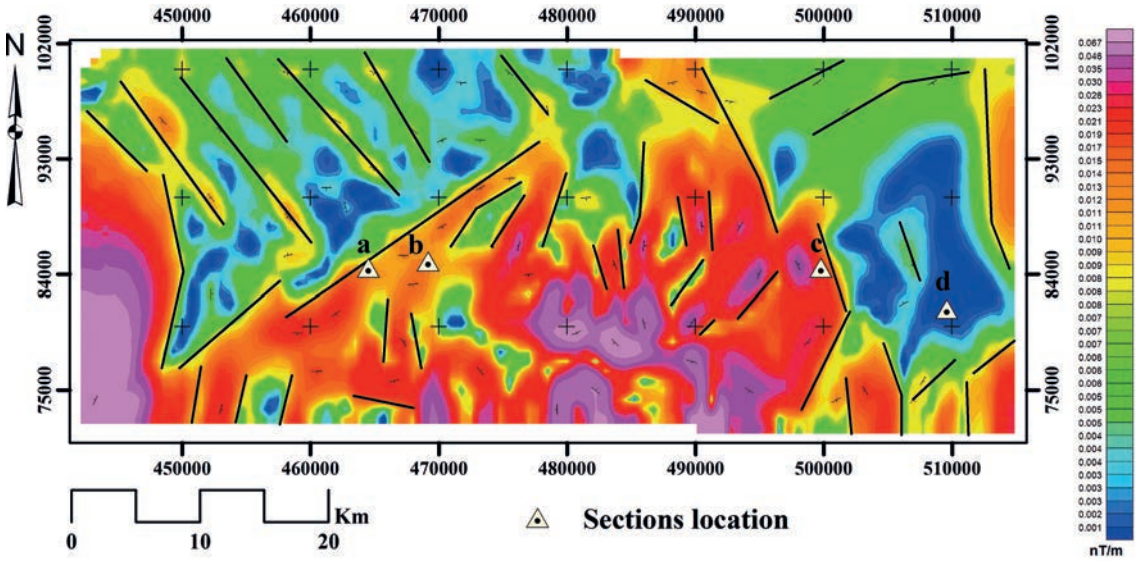

Fig. 9 - The horizontal gradient map of residual magnetic field of the Jbel Saghro northern flank: a) Boumalne section location; b) Imiter section location; c) Taghazout West section location; d) Taghazout section location.

Neoproterozoic in the Jbel Saghro. They are described as normal faults (Soulaimani *et al*., 2014; Hejja *et al*., 2020), they crosscut the basement and rarely penetrate the Palaeozoic cover (Hejja *et al*., 2020);

- the NE-SW are located in the middle of the map. Baidder (2007) describes the NE-SW family fault as responsible for the NW-SE extension, causing the Lower Cambrian rifting in the eastern Anti-Atlas.

4.2.4. The Euler deconvolution map

The Euler deconvolution has been applied to the RTP grid in order to detect and estimate the depth of magnetic faults. With a structural index *SI* equal to 0, typically used to indicate large scale faults (Harrouchi *et al*., 2016), it was possible to highlight several subsurface faults. The magnetic sources detected in the study area are frequently arranged in linear shapes. Such arrangement provides important information on the geometry and limits of the geological structures, responsible for the observed anomalies.

The map of Euler solutions (Fig. 10) shows the position of the sources and the corresponding depth. The obtained results show a compatibility with the highlighted results of horizontal gradient, the main magnetic fault systems revealed are the NE-SW and the NW-SE trending faults.

The NE-SW trending faults are mainly represented by the F1, F2, F3, F4, F5, and F6 faults, indicated on the Euler deconvolution map. These faults are mostly located at the contact between the lower Palaeozoic cover and the Neoproterozoic basement. They are characterised by a depth ranging between 500 and 1000 m, and increase toward the Palaeozoic cover (Fig. 10). They crosscut the basement outcrops and delineate the Cambrian series.

The NW-SE trending faults given by Euler's solutions are frequently detected in the north-western part of the map with a deeper effect that can reach 1500 m.

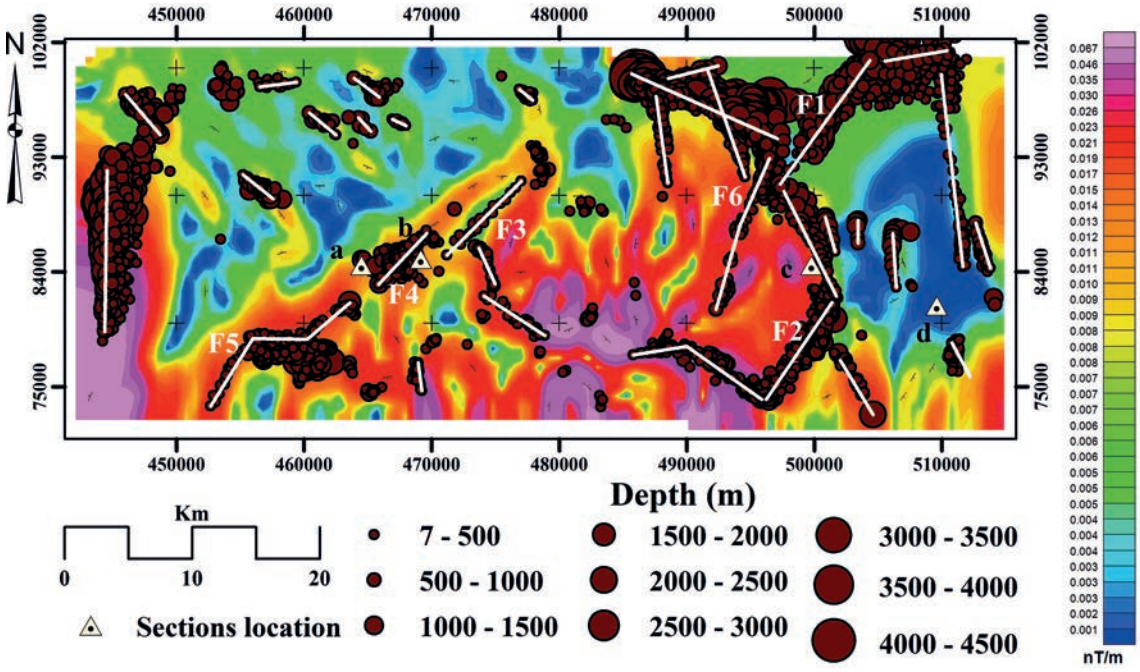

Fig. 10 - Projection of Euler's solutions on the Jbel Saghro northern flank's horizontal gradient map, showing the location of the faults in relation to the lithostratigraphic sections: a) Boumalne section location; b) Imiter section location; c) Taghazout West section location; d) Taghazout section location.

The superposition of aeromagnetic lineaments with the fault-systems, mapped by previous geological surveys (Fig. 11), allowed us to confirm the existence of a few faults that were previously mapped in the Boumalne, Imiter, and Taghazout geological maps (scale 1:50,000). Our results also enabled mapping new major subsurface faults that have not been recognised before and specify their trends and depths. Considering the depth estimated by Euler's solutions that ranges between 7 and 4500 m, this shows that these faults are buried and explains why they were not discovered at the surface level.

5. Discussion

The analysis of aeromagnetic results, in the light of the previous researches (Soulaimani *et al*., 2003; Baidder, 2007; Hejja *et al*., 2020) and the field observations carried out in this study, allowed drawing several conclusions.

The geophysical NE-SW trending faults are assumed to be responsible for the uplift of the Imiter and Boumalne regions, and the subsidence of the Taghazout region. The NW-SE trending faults are considered to be inherited from the late Neoproterozoic post-orogenic extension.

From the Late Neoproterozoic to the Lower Cambrian, a major intra-continental extension affected the Anti-Atlas domain and created subsided and uplifted areas (Fig. 12). The relatively depressed areas were invaded during the Lower Cambrian by Georgian transgression (Choubert, 1946; Soulaimani *et al*., 2003), while the high areas remained emerged.

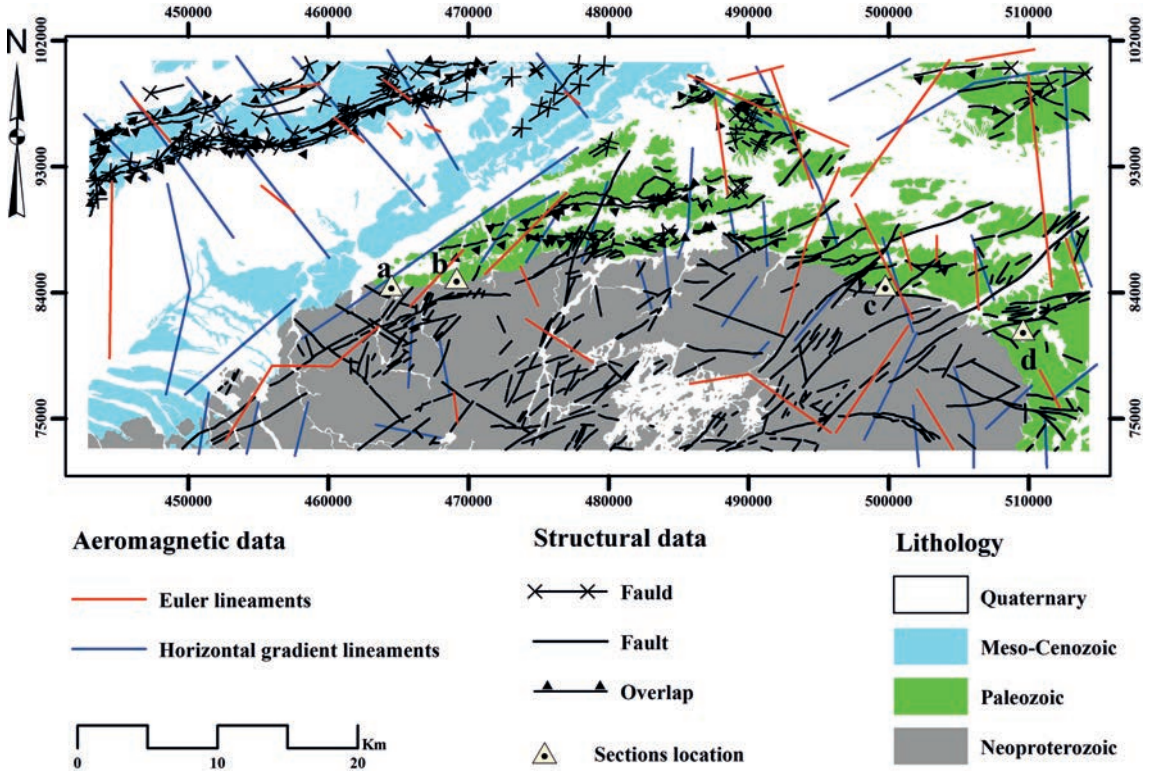

Fig. 11 - Aeromagnetic lineaments of the northern flank of Jbel Saghro superposed with fault-systems derived from geological maps of Boumalne, Imiter, and Taghazout: a) Imiter section; b) Boumalne section; c) Taghazout West section; d) Taghazout section.

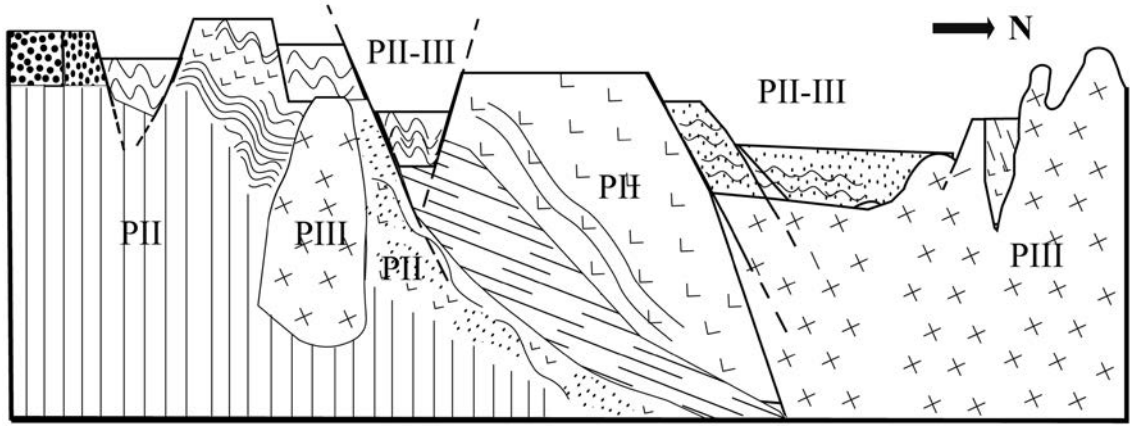

Fig. 12 - Schematic section of the Anti-Atlas Neoproterozoic basement during the Late Neoproterozoic. Legend: PII = Middle Neoproterozoic, PIII = Late Neoproterozoic (Leblanc and Lancelot, 1980).

In the eastern Anti-Atlas, the classic marker of this extension is generally the thickening of the Lower Cambrian series in the Taghazout region, and some other areas to the east of the Jbel Saghro (Fig. 5). The Imiter and Boumalne regions constitute the raised part regarding the sedimentary hiatus of the Lower Cambrian.

This hiatus has a tectonic origin, considering the Jbel Saghro geological situation with respect to the Anti-Atlas domain. To explain this phenomenon, we suggest the existence of a horst and graben system formed by the reactivation of Precambrian inherited faults. In this sense, the regions of Imiter and Boumalne are a horst while the graben exists further to the east towards the regions of Taghazout.

The Middle Cambrian formations in the Boumalne and Imiter regions are also limited and less developed compared to the Taghazout regions formations. Therefore, the schists of Taghazout West and Taghazout, resulting from the Acadian transgression (Choubert, 1946), are thicker than those of the Imiter and Boumalne sections (Fig. 5).

The lithostratigraphic logs acquired by Baidder (2007) (Fig. 5), to the east of the Jbel Saghro and to the east of the Ougnat Massif, show a thickness decreasing from east to west, while at the Jbel Saghro the thinning is from west to east. Hence, we suggest the possibility of having a graben structure between the two massifs.

6. Conclusion

The analysis of the lithostratigraphic section indicates that the Lower Cambrian deposits are absent at the western region of the Jbel Saghro, while the Middle Cambrian sediments expose a thinning trend from east towards the west. This phenomenon was produced by a tectonic origin, namely the Late Neoproterozoic - Cambrian rifting that transformed the Anti-Atlas domain into low and high areas. During the Lower Cambrian transgression, the low areas in the eastern part of the study region received an important sedimentation, whereas the high areas to the west remained emerged. After the Middle Cambrian transgression, the whole Anti-Atlas was submerged. The structural architecture of the substratum influenced the distribution of the Middle Cambrian sedimentation, once again, grabens recorded more sediments supply than horsts.

The faults, assumed to be responsible for this sedimentological architecture, are buried by latter sedimentation, so it was necessary to use aeromagnetic cartography to expose subsurface structures. The aeromagnetic data were reduced to the pole in order to be used for the horizontal gradient and Euler's deconvolution treatment. The reduction-to-pole, allowed correlating anomalies to their causative sources. The horizontal gradient highlighted several magnetic faults trending NE-SW and NW-SE, that we believe responsible for the structuring of the Jbel Saghro into horsts and grabens during the Late Neoproterozoic - Cambrian period. This explains the lateral variations of facies, and the thinning from east to west of the Lower and Middle Cambrian sedimentary series. It was possible to identify the depth of the blind faults, using the Euler deconvolution, which varies between 500 and 1500 m, the depth being low in the basement area while increasing in the cover areas.

Acknowledgements. The authors thank the reviewers for agreeing to comment on this manuscript. Our thanks also go to all those who contributed to the realisation of this work.

REFERENCES

Algouti Ab., Algouti Ah., Chbani B. and Zaim M.; 2001: *Sedimentation et volcanisme synsédimentaire de la série de base de l'adoudounien infra-cambrien à travers deux exemples de l'Anti-Atlas du Maroc*. J. Afr. Earth Sci., **32**, 541-556, doi: 10.1016/S0899-5362(02)00096-9.

Amiri A., Chaqui A., Hamdi I., Inoubli M.H., Ben Ayed N. and Tlig S.; 2011: *Role of preexisting faults in the geodynamic evolution of northern Tunisia, insights from gravity data from the Medjerda Valley*. Tectonophys., **506**, 1-10.

Azaiez H., Gabtni H., Bouyahya I., Tanfous D., Haji S. and Bedir M.; 2011: *Lineaments extraction from gravity data by automatic lineament tracing method in Sidi Bouzid Basin (central Tunisia): structural framework inference and hydrogeological implication*. Int. J. Geosci., **2**, 373-383.

Baidder L.; 2007: *Structuration de la bordure septentrionale du Craton Ouest Africain du Cambrien à l'actuel: cas de l'Anti-Atlas oriental du Maroc*. Thèse d'Etat, Université Hassan II Aïn Chock, Faculté des Sciences, Casablanca, Morocco, 210 pp.

Baranov V.; 1957: *A new method for interpretation of aeromagnetic maps: pseudogravimetric anomalies*. Geophys., **22**, 359-383.

Baranov V. and Naudy H.; 1964: *Numerical calculation of the formula of reduction to the magnetic pole*. Geophys., **29**, 67-79.

Bea F., Montero P., Haissen F., Molina J.F., Michard A., Lazaro C., Mouttaqi A., Errami A. and Sadki O.; 2016: *First evidence for Cambrian rift-related magmatism in the West African Craton margin: the Derraman Peralkaline Felsic Complex*. Gondwana Res., **36**, 423-438, doi: 10.1016/j.gr.2015.07.017.

Benssaou M. and Hamoumi N.; 2003: *Le graben de l'Anti-Atlas occidental (Maroc): contrôle tectonique de la paléogéographie et des séquences au Cambrien inférieur*. C.R. Geosci., **335**, 297-305, doi: 10.1016/S1631-0713(03)00033-6.

Blakely R.J. and Simpson R.W.; 1986: *Approximating edges of source bodies from magnetic or gravity anomalies*. Geophys., **51**, 1494-1498, doi: 10.1190/1.1442197.

Bournas N.; 2001: *Interpretation des donnees aerogeophysiques acquises au-dessus du Hoggar oriental*. Thèse Doctorat d'état, Université des Sciences et de la Technologie Houari Boumediene, Faculté des Sciences de la Terre, de la Geographie et de l'Amenagement du Territoire, Alger, Algeria, 250 pp.

Buggisch W. and Flügel E.; 1988: *The Precambrian/Cambrian boundary in the Anti-Atlas (Morocco) discussion and new results*. In: Jacobshagen V.H. (ed), The Atlas System of Morocco, Springer-Verlag, Berlin/Heidelberg, Germany, pp. 81-90, doi: 10.1007/BFb0011587.

Burkhard M., Caritg S., Helg U., Robert-Charrue C. and Soulaimani A.; 2006: *Tectonics of the Anti-Atlas of Morocco*. C.R. Geosci., **338**, 11-24, doi: 10.1016/j.crte.2005.11.012.

Choubert G.; 1946: *Aperçu de la géologie marocaine*. Rev. Géogr. Marocaine, **2-3**, 59-77.

Cordell L.; 1979: *Gravimetric expression of graben faulting in Santa Fe Country and the Espanola Basin, New Mexico*. In: Ingersoll R.V. (ed), 30th Field Conference, New Mexico Geological Society, Guidebook to Santa Fe Country, Socorro, NM, USA, pp. 59-64.

Cordell L. and Grauch V.J.S.; 1985: *Mapping basement magnetization zones from aeromagnetic data in the san Juan Basin, New Mexico*. In: Hinze W.J. (ed), The utility of regional gravity and magnetic anomaly maps, Soc. Expl. Geophys., Tulsa, OK, USA, Chapter 16, pp. 181-197, doi: 10.1190/1.0931830346.ch16.

Destombes J. and Feist R.; 1987: *Découverte du Cambrien supérieur en Afrique (Anti-Atlas central, Maroc)*. C.R. Acad. Sc., **304**, 719-724.

Destombes J., Hollard D. and Willefert S.; 1985: *Lower Palaeozoic rocks of Morocco*. In: Holland C.H. (ed), Lower Palaeozoic rocks of north-western and west-Central Africa, John Wiley and Sons Ltd, Chichester, UK, pp. 91-336.

Dufréchou G., Harris L.B. and Corriveau L.; 2013: *Tectonic reactivation of transverse basement structures in the Grenville orogeny of SW Quebec, Canada: insights from gravity and aeromagnetic data*. Precambrian Res., **241**, 61-84.

Ennih N. and Liégeois J.-P.; 2001: *The Moroccan Anti-Atlas: the West African Craton passive margin with limited Pan-African activity. Implications for the northern limit of the craton*. Precambrian Res., **112**, 289-302.

Gabtni H., Jallouli C., Mickus K. and Turki M.M.; 2013: *Geodynamics of the southern Tethyan Margin in Tunisia and Maghrebian domain: new constraints from integrated geophysical study*. Arabian J. Geosci., **6**, 271-286.

Gasquet D., Levresse G., Cheilletz A., Azizi-Samir M.R. and Mouttaqi A.; 2005: *Contribution to a geodynamic reconstruction of the Anti-Atlas (Morocco) during Pan-African times with the emphasis on inversion tectonics and metallogenic activity at the Precambrian - Cambrian transition*. Precambrian Res., **140**, 157-182, doi: 10.1016/j.precamres.2005.06.009.

Gasquet D., Ennih N., Liégeois J.-P., Soulaimani A. and Michard A.; 2008: *The Pan-African Belt*. In: Michard A., Saddiqi O., Chalouan A. and Frizon Lamotte D. (eds), Continental Evolution: the geology of Morocco, Lecture Notes in Earth Sciences, Springer, Berlin, Germany, pp. 33-64.

Geosoft Inc., 2007: *Oasis montaj*. <www.geosoft.com/media/uploads/resources/brochures/OM_b_2008_10_web.pdf>.

Gouiza M., Charton R., Bertotti G., Andriessen P. and Storms J.E.A.; 2017: *Post-Variscan evolution of the Anti-Atlas Belt of Morocco constrained from low-temperature geochronology*. Int. J. Earth Sci., **106**, 593-616, doi: 10.1007/s00531-016-1325-0.

Harrouchi L.; 2017: *Développement de méthodes analytiques et numériques de traitements et d'interprétations de données de champ de potentiel. Application a l'étude de l'In Ouzzal et des zones adjacentes*. Thèse d'etat, Faculté des sciences de la terre, de la géographie et de l'aménagement du territoire, Université des sciences et de la technologie Houari Boumedienne, Alger, Algerie, 70 pp.

Harrouchi L., Hamoudi M., Bendaoud A. and Beguiret L.; 2016: *Application of 3D Euler deconvolution and improved tilt angle to the aeromagnetic data of In Ouzzal terrane, western Hoggar, Algeria*. Arabian J. Geosci., **9**, 508, doi: 10.1007/s12517-016-2536-1.

Hejja Y., Baidder L., Ibouh H., Bba A.N., Soulaimani A., Gaouzi A. and Maacha L.; 2020: *Fractures distribution and basement-cover interaction in a polytectonic domain: a case study from the Saghro Massif (eastern Anti-Atlas, Morocco)*. J. Afr. Earth Sci., **162**, 103694, doi: 10.1016/j.jafrearsci.2019.103694.

Leblanc M. and Lancelot J.R.; 1980: *Interprétation géodynamique du domaine pan-africain (Précambrien terminal) de l'Anti-Atlas (Maroc) à partir de données géologiques et géochronologiques*. Can. J. Earth Sci., **17**, 142-155, doi: 10.1139/e80-012.

Marante A.; 2008: *Architecture et dynamique des systemes sedimentaires silico-clastiques sur la «plate-forme geante» nord-gondwanienne l'ordovicien moyen de l'Anti-Atlas Marocain, universite Michel de montaigne*. Thèse de doctorat en Science et Technologie, Science de la Terre, Université Bordeaux Montaigne, Bordeaux, France, 201 pp.

Mokhtari A.; 1993: *Nouvelles données et interprétations du massif basique de Tagmout (Jbel. Saghro, Anti-Atlas, Maroc): relations avec les granitoïdes associés*. Thèse de doctorat en Terre, Océan, Espace, Université Henri Poincaré Nancy 1, Faculté des Sciences et Techniques, Nancy, France, 251 pp.

Nait Bba A., Boujamaoui M., Amiri A., Hejja Y., Rezouki I., Baidder L., Inoubli M.H., Manar A. and Jabbour H.; 2019: *Structural modeling of the hidden parts of a Paleozoic Belt: insights from gravity and aeromagnetic data (Tadla Basin and Phosphates Plateau, Morocco)*. J. Afr. Earth Sci., **151**, 506-522.

Piqué A., Soulaimani A., Hoepffner C., Bouabdelli M., Laville E., Amrhar M. and Chalouan A.; 2007: *Geologie du Maroc*. Ed. Géode, Marrakech, Morocco, 280 pp.

Pouclet A., El Hadi H., Alvaro J.-J., Barintzeff J.-M., Benharref M. and Fekkak A.; 2018: *Review in the Cambrian volcanic activity in Morocco: geochemical fingerprints and geotectonic implications of the rifting of West Gondwana*. Int. J. Earth Sci., **107**, 2101-2123, doi: 10.1007/s00531-018-1590-1.

Raddi Y., Baidder L., Michard A. and Tahiri M.; 2007: *Variscan deformation at the northern 877 border of the West African Craton, eastern Anti-Atlas, Morocco: compression of a mosaic 878 of tilted blocks*. Bull. Soc. Géol. Fr., **178**, 343-352.

Reid A.B., Allsop J.M., Granser H., Millett A.J. and Somerton I.W.; 1990: *Magnetic interpretation in three dimensions using Euler deconvolution*. Geophys., **55**, 80-91, doi: 10.1190/1.1442774.

Soulaimani A., Bouabdelli M. and Piqué A.; 2003: *The Upper Neoproterozoic - Lower Cambrian continental extension in the Anti-Atlas (Morocco)*. Bull. Soc. Geol. Fr., **174**, 83-92, doi: 10.2113/174.1.83.

Soulaimani A., Michard A., Ouanaimi H., Baidder L., Raddi Y., Saddiqi O. and Rjimati E.C.; 2014: *Late Ediacaran-Cambrian structures and their reactivation during the Variscan and Alpine cycles in the Anti-Atlas (Morocco)*. J. Afr. Earth Sci., **98**, 94-112.

Soulaimani A., Ouanaimi H., Saddiqi O., Baidder L. and Michard A.; 2018: *The Anti-Atlas Pan-African Belt (Morocco): overview and pending questions*. C.R. Geosci., **350**, 279-288, doi: 10.1016/j.crte.2018.07.002.

Thompson D.T.; 1982: *EUDPH: a new technique for making computer-assisted depth estimates from magnetic data*. Geophys., **47**, 31-37.

Corresponding author: Assia Idrissi
Department of Earth Sciences, Faculty of Sciences, Mohamed V University
Ibn Battouta Street, Rabat, Morocco
Phone: +212 615-630-385; e-mail: idrissi.assia5@gmail.com